Marine and Petroleum Geology 27 (2010) 215–222

Contents lists available at ScienceDirect

Marine and Petroleum Geology

journal homepage: www.elsevier.com/locate/marpetgeo

Deformation bands formed during soft-sediment deformation: Observations from SE Utah

Haakon Fossen*

Department of Earth Science and Centre of Integrated Petroleum Research, University of Bergen, Allégaten 41, 5007 Bergen, Norway

ARTICLE INFO

Article history:
Received 29 August 2008
Received in revised form
21 May 2009
Accepted 19 June 2009
Available online 26 June 2009

Keywords:
Deformation bands
Permeability
Fault rocks
Subseismic deformation

ABSTRACT

Several types of syndepositional deformation structures contain strain localization structures known as disaggregation bands. Abundant field examples from Utah show that such bands can be related to vertical movements linked to loading and fluid expulsion, forming a pre-tectonic set of strain localization structures in deformed sandstones that can easily be overlooked or misinterpreted as tectonic structures in petroleum reservoirs. Plug measurements and thin-section investigations show that they have little or no influence on fluid flow. In contrast, disaggregation bands formed as a response to tectonic stress at higher confining pressures (depths) in the same lithology show up to 3–4 orders of magnitude reduction in permeability. This makes it important to distinguish between synsedimentary and tectonic deformation bands. They should also be separated because only bands formed in relation to tectonic stress can be used to predict nearness to important faults and to assess the extent of faulting in a reservoir.

1. Introduction

Deformation bands have now been described from porous sandstone formations around the world, but primarily from the Triassic–Jurassic formations of the Colorado Plateau (e.g. Davis 1999) where they were pioneered by Atilla Aydin in the late 1970's (Aydin, 1978; Aydin and Johnson, 1978, 1983). The majority of these works concern cataclastic deformation bands (bands involving grain crushing), and many are related to the Jurassic sandstones of the San Rafael Desert and the Moab area (Antonellini et al., 1994; Antonellini and Aydin, 1995; Fossen and Hesthammer, 1997; Shipton et al., 2002; Davatzes and Aydin, 2003).

It is now well known that cataclastic deformation bands represent only one of several types of deformation bands, and that the type of band depends on both rock properties and external physical conditions. It is of importance for several reasons to be able to distinguish between types of bands and predict where and under what conditions they form. One goal is to be able to retrieve information about the physical conditions during deformation from structural/petrographical observations of deformation bands. Another is to predict the type of deformation band in a reservoir based on lithological characteristics, burial depth during deformation and other geologic information. This contribution focuses on deformation bands formed shortly after deposition and how they differ from strain localization structures formed later during the burial history.

2. Deformation bands

Deformation bands are mm-thick tabular zones of localized deformation that occur in deformed porous sediments and sedimentary rocks in a variety of depositional and structural settings (Fossen et al., 2007). They do not show any continuous and mechanically weak fracture surface, although mesoscopic slip surfaces may develop in deformation band clusters (Aydin, 1978). Instead, they define a zone of deformation that is several times wider than the grain size of the host rock. The vast majority of deformation bands in naturally deformed rocks and sediments are shear bands with some compaction across them, while dilation (Du Bernard et al., 2002) and compaction bands (Molemma and Antonellini, 1996) also occur.

Several mechanisms can be operative during the formation of deformation bands (Table 1). Grain reorganization or *disaggregation* is a common non-destructive mechanism where grains roll and translate by frictional sliding along primary grain contacts. This deformation mechanism is termed particulate or *granular flow* (Table 1). When phyllosilicates are represented in the rock, a fabric may form in the band, and the band becomes a (framework) phyllosilicate band (Knipe et al., 1997). In pure quartz sandstones with a uniform grain size, disaggregation bands are more or less invisible. Only where a visually distinguishable lamination is

* Tel.: +47 55583495.
E-mail address: haakon.fossen@geo.uib.no

0264-8172/$ – see front matter © 2009 Elsevier Ltd. All rights reserved.
doi:10.1016/j.marpetgeo.2009.06.005

Table 1
Schematic overview of mechanisms operating during deformation band formation and their preferred conditions.

Granular flow	Shallow depth, low eff. stress, poor lithification
Cataclastic flow	>1 km depth, some lithification, high confining pressure
Dissolution (Qtz)	>2–3 km depth, >90 °C, locally along faults due to fluid flow
Cementation	For quartz, same as above. Calcite shallower

present may they be identifiable in the form of ductile shearing of the lamination (Fig. 1).

Breaking or crushing of grains can occur during the formation of deformation bands, giving rise to catalastic deformation bands (Aydin, 1978). Extensive grain fracturing leads to localized *cataclastic flow* (Table 1), where broken grain fragments experience frictional sliding. Cataclastic bands generally involve some compaction and porosity reduction due to reorganization of broken grains. Some bands also show evidence of *dissolution*, a mechanism which results in what is known as chemical compaction.

The variables that predetermine which mechanism is operative in a deformation band are many and not fully understood. A certain deformation depth or confining pressure is thought to be needed for cataclastic bands to form: classical cataclastic deformation bands in the Navajo and Entrada Sandstones formed at 2–3 km depth (e.g. Davatzes and Aydin, 2003) and those in Sinai at ~1.5 km depth (Rotevatn et al., 2008). The minimum depth for significant cataclasis to occur is commonly quoted at ~1 km, although the critical depth varies with other parameters such as mineralogy, grain size, sorting, porosity and grain shape. Thus, some grain breakage or flaking have been reported from more shallowly buried sediments as well (Cashman and Cashman, 2000), generally feldspar and lithic fragments rather than quartz (Rawling and Goodwin, 2003). It is emphasized that disaggregation bands can form at any depth in porous sandstone, where they appear to be promoted by high pore fluid pressure, no cementation, fine grain size and poor sorting.

3. The Courthouse area

3.1. Stratigraphic setting

The main study area is located in the footwall of the Courthouse Fault (Fossen et al., 2005), a fault segment that is linked to the Moab fault near Courthouse Rock, 26 km NW of Moab, Utah (Figs. 2, 3). The strategraphic units in the Courthouse Rock area are the Jurassic Navajo Sandstone and the overlying Entrada Sandstone (Doelling and Morgan, 2000), now referred to as the San Rafael Group in this area (Doelling, 2001) (Fig. 4). The Navajo Sandstone forms the base of the valley and is well exposed uphill from the key locality of this study. The Navajo Sandstone is a pale yellowish eolian sandstone that, together with the equivalent Aztec and Nugget sandstones, covers a significant part of the south-western USA. In the study area, the Navajo Sandstone is a fine-grained and well-sorted eolian quartz sandstone. Dune cross-stratification is well developed, with up to 6 m thick dune units. Soft-sediment deformation is seen in the uppermost part of the Navajo Sandstone, for instance near the Arches National Park visitor center, where the stratification is folded into gentle to tight folds and affected by numerous deformation bands that formed during the folding (disaggregation) and during the formation and growth of the Moab Fault.

Fig. 1. Synsedimentary disaggregation band in sand dune deposits of the Navajo Sandstone, Arches National Park, invisible in homogeneous sandstone. Displacement can be measured on selectively eroded surfaces (See Fig. 2, inset map).

The San Rafael Group consists of the Dewey Bridge, Slick Rock and Moab members, all previously regarded as the Entrada Sandstone (Fig. 4). The reddish to brownish Dewey Bridge Member is a well-stratified package of sabkha and, locally, eolian deposits considered to be equivalent to the marine Carmel Formation farther west (Blakey et al., 1988). In general, the Dewey Bridge Member consists of interbedded poorly sorted fine-grained sandstone and siltstone, with a more sandy lower part. However, in the Courthouse area a body of fine-grained fluvial sandstone occurs in the uppermost part (here referred to as the upper Dewey Bridge sandstone), separated from the overlaying Slick Rock Member by two very prominent dark brown mudstone beds a few decimeters thick (Fig. 3). The planar and undisturbed nature of these mudstone beds stand in strong contrasts to the lower contact of the upper Dewey Bridge sandstone, which conforms the lumpy and contorted bedding that dominates the underlying fine-grained Dewey Bridge layers. The massive and fine-grained upper Dewey Bridge sandstone takes up these irregularities and did so before the deposition of the planar siltstones that mark the very top of the Dewey Bridge Member.

The contorted bedding of the Dewey Bridge–Entrada interface is a synsedimentary feature that characterizes this stratigraphic level in this part of SE Utah, and a number of explanation has been suggested for its occurrence, including loading of the muddy part of the Dewey Bridge Member by the overlying upper Dewey Bridge sand, and impact-related shaking (Alvarez et al., 1998). Measured permeability in the upper Dewey Bridge sandstone varies from 28 to 67 md (TinyPerm in situ measurements and plug measurements), and porosity from 15 to 19% (helium porosity by Boyle's law technique from inch-long drill plugs, performed at ResLab in Stavanger, Norway).

The cliff-forming Slick Rock Member (Entrada Formation) is, similar to the Navajo Sandstone, a dune-sea deposit, but has a much higher content of planar interdune layers and thus represents a wetter eolian system than the Navajo. The Slick Rock has for the most part preserved its reddish color while the Navajo is bleached. The bleaching is related to chemically reducing fluids flushing through the most permeable sandstones, dissolving and removing the reddish hematite grain coating (Chan et al., 2000). The Slick Rock also contains more hematite than the underlying upper Dewey Bridge sandstone, suggesting that the permeability of the upper Dewey Bridge Member sandstone is higher. This has been confirmed by permeability measurements.

In addition to the upper Dewey Bridge and Slick Rock Members, the third dune unit exposed in the Courthouse area is the Moab Member, which is a 30 m thick eolian sandstone that is totally bleached and thus more permeable than the mostly reddish Slick Rock Member. The Moab Member forms the rim of the Courthouse Rock and similar rock formations in the area. It is also characterized by uplift/cooling-related joints that are scarce or absent in the underlying units.

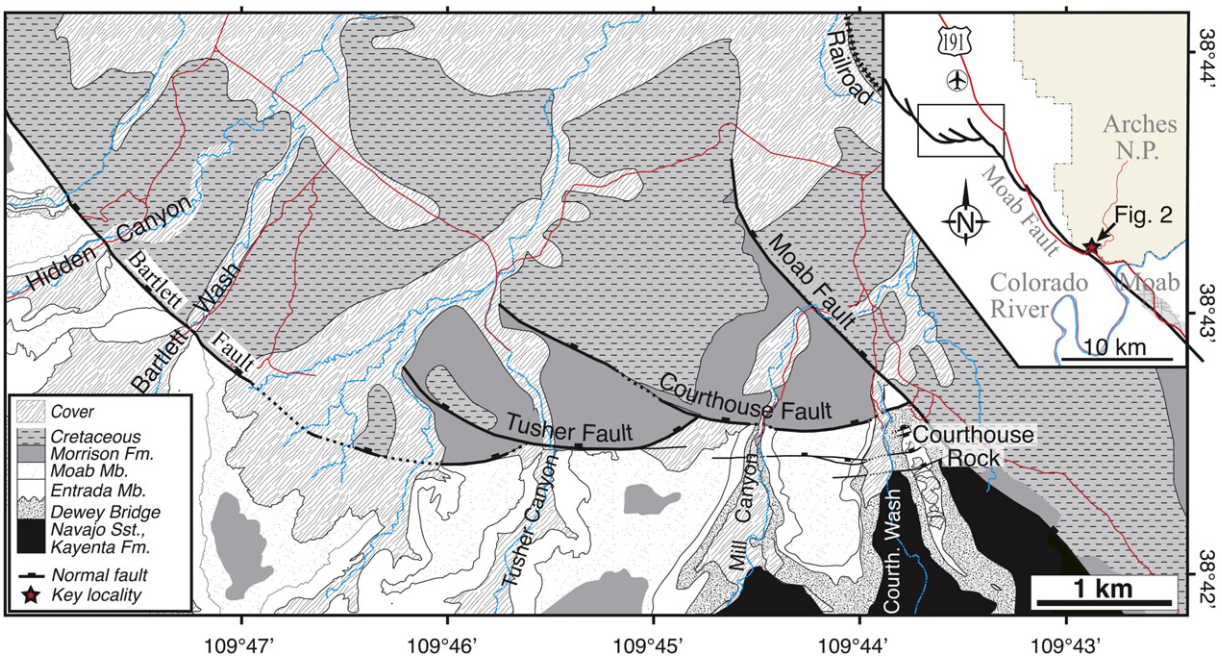

Fig. 2. Geologic map of the Courthouse Rock and surrounding areas. Modified from Doelling and Morgan (2000).

3.2. Structural setting

The Courthouse-Tusher-Bartlett faults form a linked fault system that links to the Moab Fault in the Courthouse area. The fault system is related to salt tectonics and has a history of activity that dates back to at least 60 Ma (Solum et al., 2005). The Courthouse Fault shows decreasing displacement toward the Moab Fault, reaching ~60 m at the branch point. A few minor faults transect Courthouse Rock and run parallel to the Courthouse Fault (Figs. 2, 3). The small-scale deformation features related to the formation and growth of the Moab and Courthouse-Tusher-Bartlett faults are manifested by cataclastic and some disaggregation deformation bands striking more or less parallel to the faults, extension fractures and slip surfaces that cross-cut the cataclastic deformation bands (Davatzes and Aydin, 2003; Johansen et al., 2005). These structures are easily distinguished from the older, synsedimentary deformation bands that are the primary aim of this study.

The Courthouse area is of particular interest because of the many types of deformation structures found in this small area. Locally, an evolution from classical cataclastic deformation bands via thin cataclastic deformation bands to shear fractures has been described (Davatzes et al., 2005; Johansen et al., 2005). All of these structures formed during the evolution of the Moab fault system at 2–3 km depth (Fig. 5), and can be related to changing physical properties and stress conditions of the rock during faulting (Davatzes et al., 2005; Johansen et al., 2005). Subsequently, regionally persistent fracture sets formed as these rocks cooled and decompressed during the late Cenozoic uplift history of the Colorado Plateau (e.g. Foxford et al., 1998). This rather comprehensive

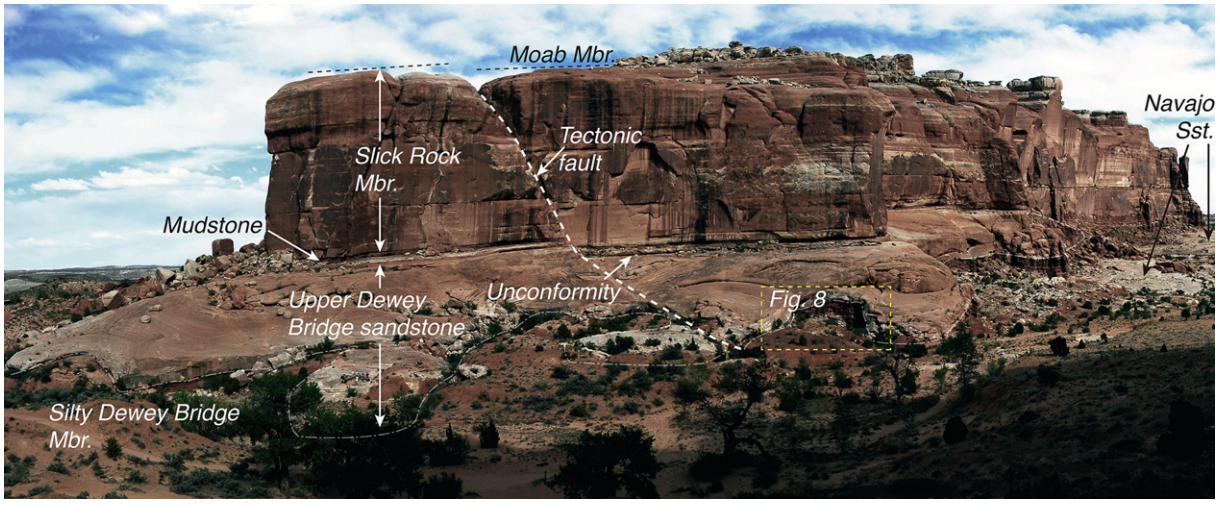

Fig. 3. Courthouse Rock and its stratigraphy. Note contorted nature of the silty lower Dewey Bridge Member.

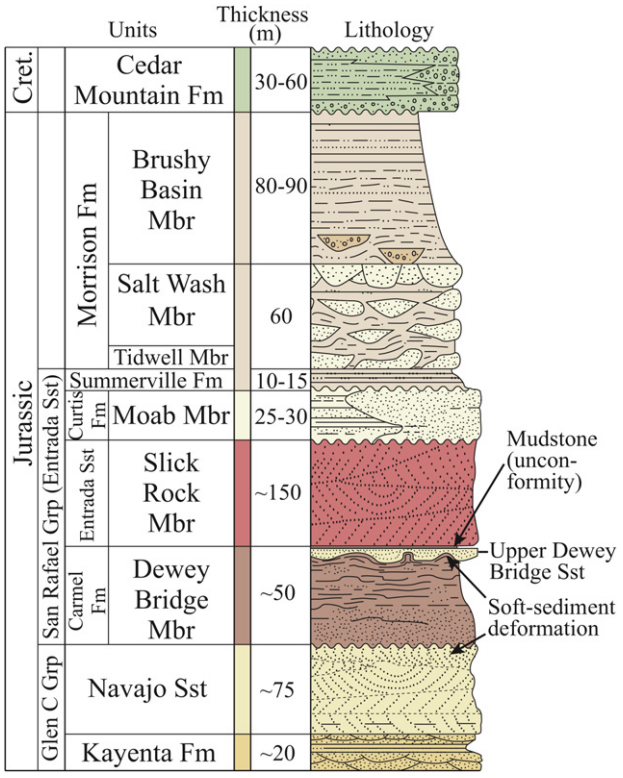

Fig. 4. Stratigraphic column of the Courthouse area. Modified from Doelling and Morgan (2000).

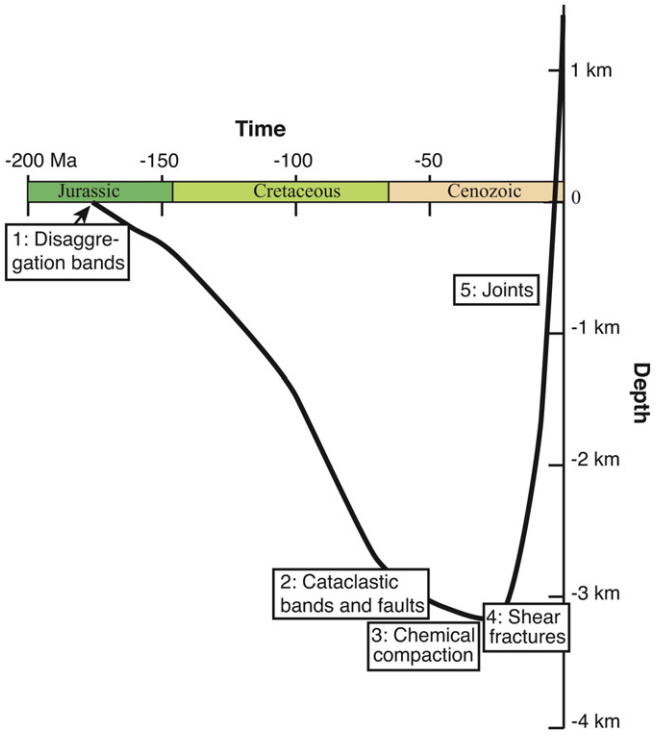

Fig. 5. Subsidence curve, based on the stratigraphic column in the Courthouse area (Doelling and Morgan, 2000) and the Book Cliffs area (Doelling, 2001). Formation of small-scale structures is indicated.

selection of brittle strain localization structures can be related to a relatively simple history of sedimentation, burial, tectonic deformation and uplift, a history that it shears with many other sedimentary rock units in the world.

4. Synsedimentary folds and disaggregation bands

4.1. Folds

Several syndepositional folds with up to 10 m amplitude and wave lengths in the order of 60–70 m occur around the mudstone–sandstone interface of the Dewey Bridge Member at the base of Courthouse Rock (Figs. 3 and 6). The folds disappear some 250 m south of the Courthouse Fault, but folds occur at this stratigraphic level elsewhere in the Moab area. However, the folds in the Courthouse area are particularly well developed. Their three-dimensional geometries are difficult to map, but the outcrop pattern and bedding orientations give a clear indication that they are highly non-cylindrical, possibly close to dome-and-basin structures. Meter-scale circular bedding traces on subhorizontal surfaces at several stratigraphic levels within the upper Dewey Bridge sandstone support this view. Some of these are evidently truncated by younger sand layers (Fig. 6), indicating that the fold structures amplified during deposition of the upper Dewey Bridge sandstone. Such observations seem incompatible with the impact theory (Alvarez et al., 1998) as an explanation for how these particular fold structures formed.

4.2. Disaggregation bands

A dense array of deformation bands occurs in the fluvial upper Dewey Bridge sandstone. The deformation bands are for the most part exposed on gently dipping surfaces where they can be seen to offset the sandstone laminas. In more homogeneous parts of the sandstone where lamination is not visually exposed, some deformation bands can be discerned by a change in color or slightly positive or negative relief. In some low-permeable layers the bands are somewhat darker brownish than their host rock due to a concentration of oxides. In other layers bands are more or less invisible, making it difficult to map them in detail.

The deformation bands are very difficult to identify under the microscope, as there is no sign of grain crushing or obvious porosity change, and the only visual expression being a weak, local fabric in some cases (Fig. 7). Some grain contact dissolution is seen in both the bands and the host rock, and is regarded as a diagenetic feature related to the Cenozoic part of the burial history. The complete absence of grain fracturing is distinctly different from cataclastic deformation bands associated with tectonic faults in the area, suggesting that mechanism operative during deformation is rigid grain rolling and non-destructive frictional sliding along grain–grain contacts, i.e. granular flow with no grain fracture (e.g. Mandl, 2000). Thus, the bands classify as disaggregation bands (Fossen et al., 2007).

Most of the deformation bands are steeply dipping (Fig. 8), showing normal and locally reverse displacement. Apparent displacements up to tens of centimeters are seen on the shallowly dipping outcrop surfaces, whereas true displacement is some centimeters in most cases, less commonly up to ~10 cm. Although their complete length and height are rarely mappable they are confined to the upper Dewey Bridge sandstone. The bands are also unevenly distributed within the sandstone, with high densities in the lower part and practically none in the upper part. Furthermore, there is a positive correlation between band density and the curvature of the lower contact, as portrayed in Fig. 6. In particular, the bands are concentrated at the flanks of the mud structure

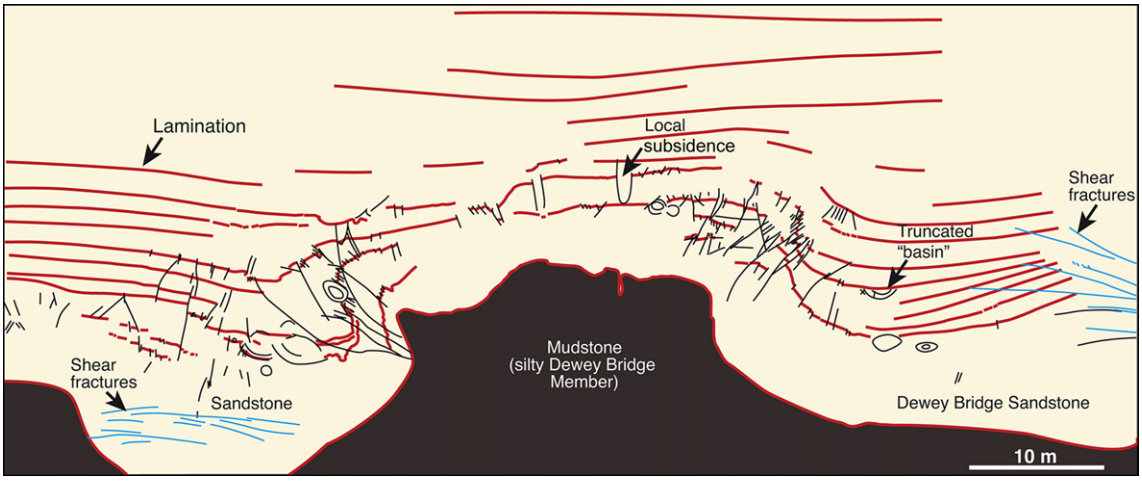

Fig. 6. Drawing of sand-shale mobilization and related deformation structures in the sandstone, based on photographs.

where strain related to fold growth is at its highest. This observation shows that the deformation bands are expressions of soft-sediment deformation connected with loading of sand on the muddy Dewey Bridge Member, as illustrated schematically in Fig. 9. The reverse offset of the bands along the flanks of the fold can be explained by rotation of steep normal-offset bands (Fig. 9), but could also be generated as reverse structures during growth of the structure, a feature seen along the upper flanks of some salt diapirs (e.g. Davison et al., 1996).

4.3. Permeability

In addition to permeability estimates by means of a TinyPerm II handheld permeameter, permeability was measured along inch-long plugs that were drilled out of the sandstones and brought to ResLab, Norway for standard determination of Klinkenberg-corrected gas permeability. Plug measurements of sandstone with and without deformation bands show no significant difference in neither porosity (plugs from the band yield porosity values that fall within the 28–67 md range found for the host rock) or permeability (Fig. 10). This is closely related to the deformation mechanism (non-cataclastic granular flow): the shifting of grains has lead to minor if any changes in permeability and porosity. A slight contrast in permeability could have been present before burial due to dilation or compaction of grains, but any such difference has been reduced during compaction to a level that is difficult to identify.

This situation could have been different if phyllosilicate minerals such as clays and micas had been present. Alignment of phyllosilicate minerals in disaggregation bands from the Middle Jurassic North Sea reservoirs, which deformed at shallow depth shortly after deposition, causes reductions in permeability by 0–6 orders of magnitude (Fisher and Knipe, 2001). However, the permeability across such bands is commonly seen to be highly variable along the band due to variations in the local source of phyllosilicates (Torabi and Fossen, 2009).

Disaggregation bands in the damage zone of the Bartlett fault segment of the Moab Fault in the nearby Bartlett Wash were also explored, and plug data indicate up to 3–4 orders of magnitude reduction in permeability as compared to their respective host

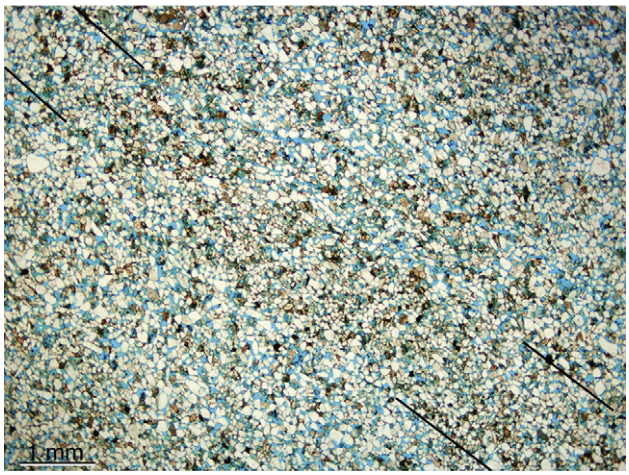

Fig. 7. Typical disaggregation deformation band of the Dewey Bridge Mbr., running diagonally across the picture.

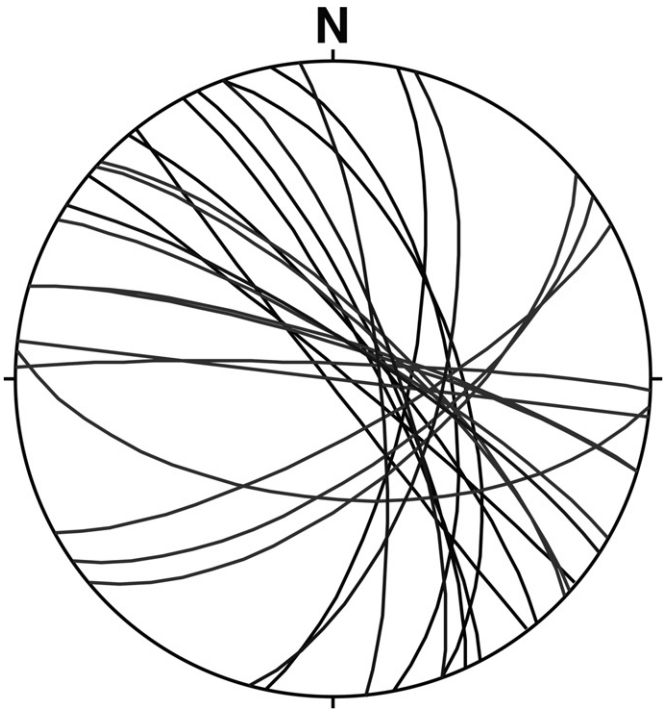

Fig. 8. Orientations of deformation bands in the small area outlined in Fig. 3. The plot shows that most bands are steep with a preferred NW-SE trend, but the range in orientation is wide.

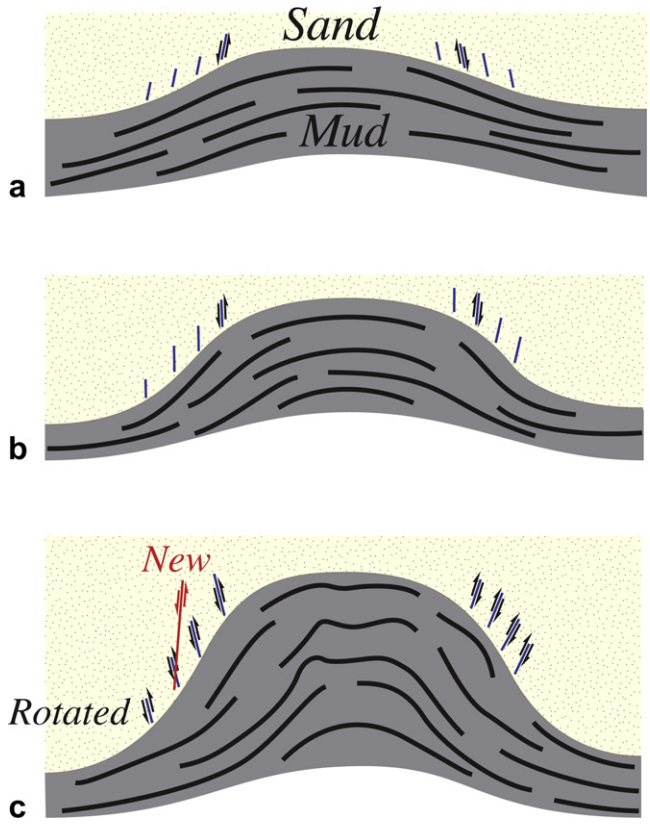

Fig. 9. Evolutionary model of synsedimentary mud mobilization and deformation band formation.

rocks. These bands are located in fine-grained sandstones in the Slick Rock Formation and formed at 2–3 km depth together with cataclastic deformation bands in coarser-grained sandstone beds.

4.4. Displacement–Length relations

Displacement–length (D_{max}–L) relationships of faults populations have been widely discussed in the literature (e.g. Cowie and Scholz, 1992; Dawers et al., 1993; Watterson et al., 1996). The scaling relationship between D_{max} and L is expressed by the power-law relation:

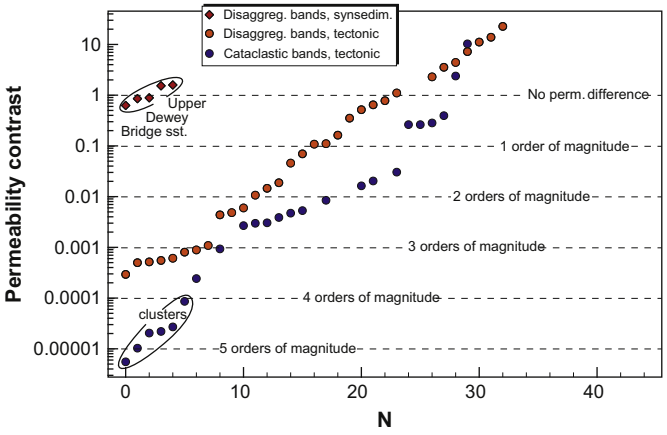

Fig. 10. Permeability data (plug measurements) from the Courthouse area and related locations in the ergs of SE Utah. According to the measurements, the synsedimentary bands discussed in this paper have no influence on the permeability structure of the rock.

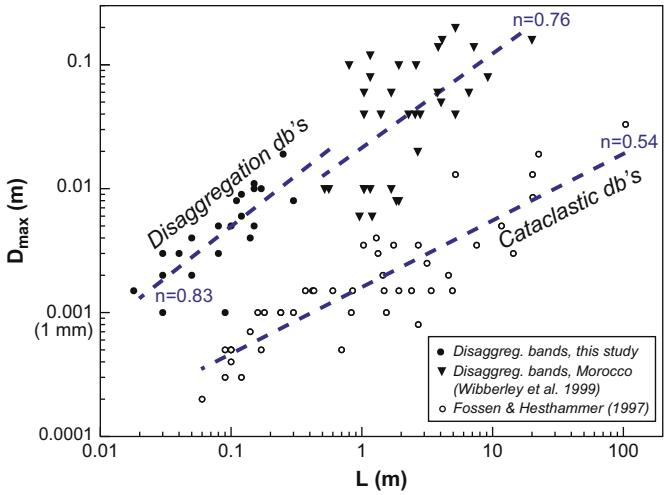

Fig. 11. Displacement versus length of deformation bands for disaggregation bands from porous sandstones of the Moab area and Morocco (Wibberley and Petit, 1999), as compared to cataclastic bands from the Entrada Sandstone west of the study area (Fossen & Hesthammer 1997). db = Deformation bands.

$$D_{max} = \gamma L^n$$

where the exponent $n \sim 1$ for faults, i.e. faults generally show a linear dependence of D_{max} and L (in which case the constant γ equals D_{max}/L). A D_{max}–L relationship was established for cataclastic deformation bands in the Entrada Sandstone in the San Rafael Desert some 85 km west of Courthouse Rock (Fossen and Hesthammer, 1997). The deformation band data showed a scaling law where $n = 0.5$, i.e. quite different from that established for faults and slip surfaces ($n = 1$). In particular, it was found that for a given displacement, the cataclastic deformation bands were longer than predicted by established fault D_{max}–L data by around 2 orders of magnitude.

Reliable D_{max}–L data were difficult to obtain from the syndepositional disaggregation bands in the Courthouse Rock area, but were collected from the stratigraphically underlying Navajo Sandstone in the nearby Arches National Park (Fig. 2, inset map). Also here disaggregation bands formed during soft-sediment deformation of the sand shortly after deposition, as can be seen by the folding of the Navajo sand dunes prior to deposition of the overlying Dewey Bridge Member. The data are plotted in Fig. 11, where they clearly define a trend. They scale differently from the cataclastic deformation bands, and their n-exponent ($\sim$0.83) is closer to that defined by faults (around 1.0).

5. Discussion

The observations from the Courthouse area demonstrate how a sand (stone) can accommodate strain through the operation of different deformation mechanisms and structures, depending on external and internal conditions. While individual differences occur, the sequence of small-scale deformation structures in the sandstones of the Courthouse area is characteristic for many sedimentary basins: 1) syndepositional disaggregation bands at very shallow depths; 2) cataclastic and disaggregation deformation bands at 2–3 km depth, formed as precursors to tectonic faults; 3) slip surfaces and minor faults, and 4) extension fractures formed during uplift.

Among these, early disaggregation bands are numerous but overlooked in many cases. They can form due to loading or vertical passage of water released during physical compaction, as

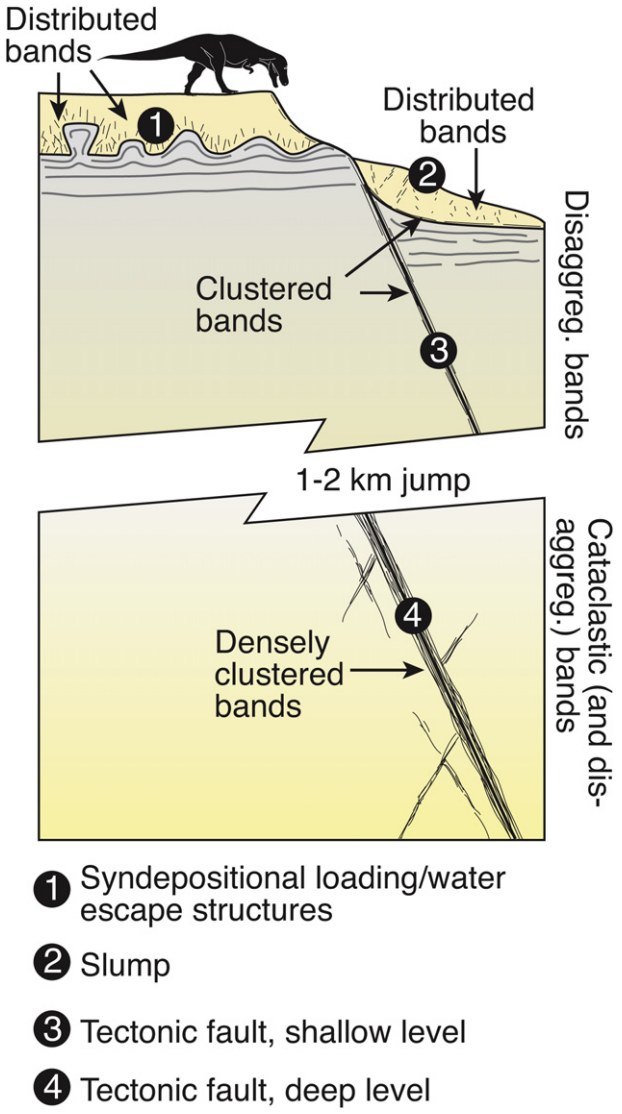

Fig. 12. Deformation bands related to nontectonic near-surface processes (1 and 2) and tectonic faults at different depths (3 and 4).

demonstrated above, or due to a hydrostatic head of water, as for example on an alluvial fan (e.g. Maltman and Bolton, 2003). Furthermore, gravitational instabilities on delta slopes and fault scarps are a likely cause of disaggregation bands. Such structures must be expected to occur frequently in silisiclastic reservoirs, for instance in the slumped east flank of rotated major fault blocks in the North Sea (Coutts et al., 1996; Hesthammer and Fossen, 1999).

Table 2
Schematic (and simplified) overview of characteristic features and properties of syndepositional (soft-sediment) and tectonic (faulting-related) deformation bands.

Synsedimentary bands	Tectonic bands
Distributed	Clustered
Disaggregation, no cataclasis	Disaggregation + cataclasis (at >1 km)
Associated with soft-sed. structures	Associated with tectonic faults
Variable orientations common	Consistent orientations, conjugate sets common
Little or no permeability reduction	Perm reduction up to several orders of magnitude
Normal D_{max}–L ratios	Low D_{max}–L ratios (long with small offsets)

5.1. Effect on fluid flow

The shallow-depth deformation structures discussed in this article differ from other deformation bands in that they do not involve grain fracturing (cataclasis) or significant porosity change. This influences their petrophysical properties: their porosity and permeability structure are mainly controlled by the amount of phyllosilicates present (Fisher and Knipe, 2001) and any simultaneous or subsequent dissolution/cementation within or along the bands (Hesthammer et al., 2002). In the (near) absence of phyllosilicates, as in the present case, they have no significant influence on fluid flow during migration or production of oil and gas.

This situation is different for bands that form deeper in a sedimentary basin. It is worth noting that disaggregation bands in the damage zone of the Bartlett Fault in the nearby Bartlett Wash (Fig. 2) show reductions in permeability up to 3–4 orders of magnitude as compared to their respective host rocks (open symbols in Fig. 10). These bands are located in fine-grained interdune sandstones Slick Rock Formation. The reason why these tectonic disaggregation bands, which become cataclastic as they enter better sorted medium-grained sand layers, show permeability reduction is related to better grain packing and concentration of iron (hydr)oxides within the bands. In addition, local crushing of grains may have an effect.

5.2. Clustering and displacement

Many disaggregation bands formed at shallow depths show maximum displacements in excess of the 0–3 cm commonly seen on cataclastic bands (Hesthammer and Fossen, 2001, Fossen and Hesthammer, 1997). The data presented above (Fig. 11) indicate that, for a given displacement, disaggregation bands are considerably shorter than cataclastic bands, i.e. they have a higher D_{max}/L ratio. Their displacements also scale differently with respect to length, with a steeper slope (n) in D_{max}–L space (Fig. 11). This is possibly related to deformation mechanism; grain fracturing causes more effective locking of grains than does granular flow and thus promotes strain hardening (Underhill and Woodcock, 1987; Aydin and Johnson, 1978, 1983). Strain hardening during the formation of cataclastic deformation bands is also the general explanation for the formation of deformation band cluster zones along and around faults. Even disaggregation bands associated with tectonic faults tend to form clusters associated with faults (slip surfaces), even though the role of strain hardening is unknown in this case.

Although tectonic disaggregation bands do cluster around faults even at shallow depths (slump detachments and tectonic faults in upper part of Fig. 12) (Hesthammer and Fossen, 2001), they do not develop the wide and high-density clusters observed in cataclastic deformation bands (lower part of Fig. 12) (Johansen and Fossen, 2008). The shallowly formed bands studied in this work (1 in Fig. 12) show very little clustering as they accommodate strain distributed over a large volume of rock: localization to form a fault is not compatible with the boundary conditions. Hence there are different degrees of band clustering associated with shallow-level deformation structures.

5.3. Concluding remarks

Early disaggregation bands are commonly neglected (Maltman, 1988) or misinterpreted as tectonic structures in spite of the fact that disaggregation bands that form during or shortly after deposition are quite common in many sands and sandstones. In addition to the loading structures described here, gravitational instabilities on delta slopes and fault block crests are a likely cause of disaggregation bands. Such structures must be expected to occur

frequently in silisiclastic reservoirs, for instance in the slumped east flank of rotated major fault blocks in the North Sea (Coutts et al., 1996; Hesthammer and Fossen, 1999).

Any evidence of meso- and macroscale slumping or contorted bedding from seismic or well data should be taken as an indication of possible small-scale disaggregation-type deformation bands in the reservoir at these levels. These bands should be separated from bands related to tectonic faulting, and important differences between deformation bands related to soft-sediment deformation and tectonic faulting are schematically summarized in Table 2. An important difference is that tectonic bands always cluster and define the damage zone on each side of the fault core in highly porous rocks (e.g. Aydin, 1978; Fossen et al., 2007). If the fault-related bands formed after significant burial, differences in permeability can be expected. Combined with their tendency to cluster, such permeability contrasts could influence fluid flow, implying that separation between the two types of bands could be important. Separation is also important for interpretation of tectonic regime; disaggregation bands related to gravitational or fluid expulsion-controlled processes tend to show a wider range of orientations, not conjugate and strike-parallel to faults as is the case with many fault-associated bands (Aydin, 1978; Underhill and Woodcock, 1987; Johansen and Fossen, 2007; Wibberley and Petit, 2007). Furthermore, they can be reverse without implying a regional contractional regime, as exemplified by the examples presented from SE Utah.

References

Alvarez, W., Staley, E., O'Connor, D., Chan, M.A., 1998. Synsedimentary deformation in the Jurassic of southeastern Utah—a case of impact shaking? Geology 26, 579–582.

Antonellini, M., Aydin, A., 1995. Effect of faulting on fluid flow in porous sandstones: geometry and spatial distribution. AAPG Bulletin 79, 642–671.

Antonellini, M.A., Aydin, A., Pollard, D.D., 1994. Microstructure of deformation bands in porous sandstones at Arches National Park, Utah. Journal of Structural Geology 16, 941–959.

Aydin, A., 1978. Small faults formed as deformation bands in sandstone. Pure and Applied Geophysics 116, 913–930.

Aydin, A., Johnson, A.M., 1978. Development of faults as zones of deformation bands and as slip surfaces in sandstones. Pure and Applied Geophysics 116, 931–942.

Aydin, A., Johnson, A.M., 1983. Analysis of faulting in porous sandstones. Journal of Structural Geology 5, 19–31.

Blakey, R.C., Peterson, F., Kocurek, G., 1988. Synthesis of late Paleozoic and Mesozoic eolian deposits of the Western Interior of the United States. Sedimentary Geology 56, 3–125.

Cashman, S., Cashman, K., 2000. Cataclasis and deformation-band formation in unconsolidated marine terrace sand, Humboldt County, California. Geology 28, 111–114.

Chan, M.A., Parry, W.T., Bowman, J.R., 2000. Diagenetic hematite and manganese oxides and fault-related fluid flow in Jurassic sandstones, southeastern Utah. American AAPG Bulletin 84, 1281–1310.

Coutts, S.D., Larsson, S.Y., Rosman, R., 1996. Development of the slumped crestal area of the Brent reservoir, Brent Field: an integrated approach. Petroleum Geoscience 2, 219–229.

Cowie, P.A., Scholz, C.H., 1992. Displacement–length scaling relationship for faults: data synthesis and discussion. Journal of Structural Geology 14, 1149–1156.

Davatzes, N.C., Aydin, A., 2003. Overprinting faulting mechanisms in high porosity sandstones of SE Utah. Journal of Structural Geology 25, 1795–1813.

Davatzes, N.C., Eichhubl, P., Aydin, A., 2005. Structural evolution of fault zones in sandstone by multiple deformation mechanisms: Moab fault, southeast Utah. GSA Bulletin 117, 135–148.

Davis, G.H., 1999. Structural geology of the Colorado Plateau Region of southern Utah. GSA Special Paper 342, 1–157.

Davison, I., Alsop, I., Blundell, D., 1996. Salt tectonics: some aspects of deformation mechanics. In: Davison, I., Alsop, I., Blundell, D. (Eds.), Salt Tectonics. Geological Society of London Special Publication, vol. 100, pp. 1–10.

Dawers, N.H., Anders, M.H., Scholz, C.H., 1993. Growth of normal faults: displacement–length scaling. Geology 21, 1107–1110.

Doelling, H.H., 2001. Geologic map of the Moab and eastern part of the San Rafael Desert 30′ × 60′ quadrangles, Grand and Emery Counties, Utah, and Mesa County, Colorado. Utah. Geological Survey Map, 180.

Doelling, H.H., Morgan, C.D., 2000. Geologic map of the Merrimac Butte quadrangle, Grand County, Utah. Utah. Geological Survey Map, 178.

Du Bernard, X., Eichhubl, P., Aydin, A., 2002. Dilation bands: a new form of localized failure in granular media. Geophysical Research Letters 29, 2176–2179.

Fisher, Q.J., Knipe, R.J., 2001. The permeability of faults within siliciclastic petroleum reservoirs of the North Sea and Norwegian Continental Shelf. Marine and Petroleum Geology 18, 1063–1081.

Fossen, H., Hesthammer, J., 1997. Geometric analysis and scaling relations of deformation bands in porous sandstone. Journal of Structural Geology 19, 1479–1493.

Fossen, H., Johansen, S.E., Hesthammer, J., Rotevatn, A., 2005. Fault interaction in porous sandstone and implications for reservoir management; examples from southern Utah. AAPG Bulletin 89, 1593–1606.

Fossen, H., Schulz, R.A., Shipton, Z.K., Mair, K., 2007. Deformation Bands in Sandstone – a Review, vol. 164. The Geological Society, London, pp. 755–769.

Foxford, K.A., Walsh, J.J., Watterson, J., Garden, I.R., Guscott, S.C., Burley, S.D., 1998. Structure and content of the Moab fault zone, Utah, USA, and its implications for fault seal prediction. Geological Society of London Special Publications 147, 87–103.

Hesthammer, J., Bjørkum, P.A., Watts, L.I., 2002. The effect of temperature on sealing capacity of faults in sandstone reservoirs: examples from the Gullfaks and Gullfaks Sør fields, North Sea. AAPG Bulletin 86, 1733–1751.

Hesthammer, J., Fossen, H., 1999. Evolution and geometries of gravitational collapse structures with examples from the Statfjord Field, northern North Sea. Marine and Petroleum Geology 16, 259–281.

Hesthammer, J., Fossen, H., 2001. Structural core analysis from the Gullfaks area, northern North Sea. Marine and Petroleum Geology 18, 411–439.

Johansen, S.E., Fossen, H., 2008. Internal geometry of fault damage zones in siliclastic rocks. In: Wibberley, C.A.J., Kurz, W., Imber, J., Holdsworth, R.E., Collettini, C. (Eds.), The Internal Structure of Fault Zones: Implications for Mechanical and Fluid-flow Properties. Geological Society of London Special Publication, vol. 299, pp. 35–56.

Johansen, T.E.S., Fossen, H., Kluge, R., 2005. The impact of syn-kinematic porosity reduction on damage zone architecture in porous sandstone; an outcrop example from the Moab Fault, Utah. Journal of Structural Geology 27, 1469–1485.

Knipe, R.J., Fisher, Q.J., Clennell, M.R., Farmer, A.B., Harrison, A., Kidd, B., McAllister, E., Porter, J.R., White, E.A., 1997. Fault seal analysis: successful methodologies, application and future directions. In: Møller-Pedersen, P., Koestler, A.G. (Eds.), Hydrocarbon Seals: Importance for Exploration and Production. Special Publication of the Norwegian Petroleum Society, vol. 7. Elsevier, pp. 15–40.

Maltman, A.J., 1988. The importance of shear zones in naturally deformed wet sediments. Tectonophysics 145, 163–175.

Maltman, A.J., Bolton, A., 2003. How sediments become mobilized. In: Van Ransbergen, P., Hillis, R.R., Maltman, A.J., Morley, C.K. (Eds.), Subsurface Sediment Mobilization. Geological Society of London Special Publication, vol. 216, pp. 9–20.

Mandl, G., 2000. Faulting in brittle rocks. an introduction to the mechanics of tectonic faults. Springer, Berlin, 434 pp.

Mollema, P.N., Antonellini, M.A., 1996. Compaction bands: a structural analog for anti-mode I cracks in aeolian sandstone. Tectonophysics 267, 209–228.

Rawling, G.C., Goodwin, L.B., 2003. Cataclasis and particulate flow in faulted, poorly lithified sediments. Journal of Structural Geology 25, 317–331.

Rotevatn, A., Torabi, A., Fossen, H., Braathen, A., 2008. Slipped deformation bands: a new type of cataclastic deformation bands in Western Sinai, Suez Rift, Egypt. Journal of Structural Geology 30, 1317–1331.

Shipton, Z.K., Evans, J.P., Robeson, K., Forster, C.B., Snelgrove, S., 2002. Structural heterogeneity and permeability in faulted aeolian sandstone: implications for subsurface modelling of faults. AAPG Bulletin 86, 863–883.

Solum, J.G., van der Pluijm, B., Peacor, D.R., 2005. Neocrystallization, fabrics and age of clay, minerals from an exposure of the Moab Fault, Utah. Journal of Structural Geology 27, 1563–1576.

Torabi, A., Fossen, H. 2009. Variation of microstructure and petrophysical properties along deformation bands. AAPG Bulletin 93.

Underhill, J.R., Woodcock, N.H., 1987. Faulting mechanisms in high-porosity sandstones: New Red Sandstone, Arran, Scotland. In: Jones, M.E., Preston, R.M.F. (Eds.), Deformation of Sediments and Sedimentary Rocks. Geological Society of London Special Publication, 29, pp. 91–105.

Watterson, J., Walsh, J.J., Gillespie, P.A., Easton, S., 1996. Scaling systematics of fault sizes on a large-scale range fault map. Journal of Structural Geology 18, 199–214.

Wibberley, C.A.J., Petit, J.-P., Rives, T., 1999. Mechanics of high displacement gradient faulting prior to lithification. Journal of Structural Geology 21, 251–257.

Wibberley, C.A.J., Petit, J.-P., Rives, T., 2007. The mechanics of fault distribution and localization in high-porosity sands, Province, France. In: Lewis, H., Couples, G.D. (Eds.), The Relationship Between Damage and Localization. Geological Society of London Special Publication, vol. 289, pp. 19–46.